Contents lists available at ScienceDirect

Global Ecology and Conservation

journal homepage: www.elsevier.com/locate/gecco

Original research article

Bull shark (*Carcharhinus leucas*) exclusion properties of the sharksafe barrier and behavioral validation using the ARIS technology

CrossMark

Craig P. O'Connell [a,b,*], Saang-Yoon Hyun [a,c], Chris B. Rillahan [a], Pingguo He [a]

[a] School for Marine Science and Technology, University of Massachusetts Dartmouth, 706 South Rodney French Boulevard, New Bedford, MA 02744, USA
[b] O'Seas Conservation Foundation, Bronx, NY, USA
[c] Department of Marine Biology, Pukyong National University, Busan, Republic of Korea

ARTICLE INFO

ABSTRACT

Magnetic deterrents have recently been employed to assess their ability to reduce elasmobranch mortality in beach nets. With previous studies exhibiting promise, the present study examined the ability of a magnetic barrier technology, known as the Sharksafe Barrier, to exclude bull sharks (*Carcharhinus leucas*) from bait, and how behavioral interactions may change with variations in environmental and biological factors. Generalized linear mixed model analyses based on 114, 30-min trials illustrate that all interacting *C. leucas* were successfully excluded from baited procedural control and magnetic regions (i.e. zero entrances through either region). Avoidance and pass around frequencies significantly differed from the control region and were based on situational context. To enhance behavioral analysis techniques, an Adaptive Resolution Imaging Sonar (ARIS) was employed which revealed that *C. leucas* distance from and swim speed associated with the magnetic barrier region were significantly greater than those associated with the procedural control region. This study demonstrates the Sharksafe barrier's effectiveness in excluding *C. leucas* from baited regions, regardless of variations in biological and/or environmental parameters. While other bather protection systems (e.g. beach nets and drumlines) continue to be used, this study exhibits promise that the Sharksafe barrier can be an eco-friendly alternative to beach nets.
© 2014 The Authors. Published by Elsevier B.V. This is an open access article under the CC BY-NC-ND license (http://creativecommons.org/licenses/by-nc-nd/3.0/).

1. Introduction

Elasmobranchs possess electroreceptors, the ampullae of Lorenzini, which have been demonstrated to serve a variety of functions including detecting conspecifics (Tricas et al., 1995), predators (Sisneros et al., 1998), prey-associated electric fields (Kajiura and Holland, 2002), and presumably the Earth's magnetic field (Kalmijn, 1974; Klimley, 1993; Paulin, 1995; Klimley et al., 2002; Meyer et al., 2005). The mechanism behind elasmobranch electric field detection is widely reported in the literature (e.g. Kalmijn, 1966, 1971, 1974, 1982, 2000; Bastian, 1994; Tricas and Sisneros, 2004). The ampullae of

---

* Corresponding author at: School for Marine Science and Technology, University of Massachusetts Dartmouth, 706 South Rodney French Boulevard, New Bedford, MA 02744, USA.
E-mail address: oseasfdn@gmail.com (C.P. O'Connell).

Lorenzini is composed of subcutaneous canals which project to surface pores located around the cephalic region or pectoral fins of elasmobranchs. These canals terminate at an innervated ampulla. Each ampulla and canal is filled with a low resistance hydrogel (Brown et al., 2005). Upon encountering an electrical stimulus, such as that produced by prey, the voltage potential existing at the pore surface differs from the internal potential. This difference elicits a neurological impulse that is sent to the brain where the stimulus is perceived (Kalmijn, 1974).

In contrast to the well-reported and presumably well understood electric field detection mechanism in elasmobranchs, there remains debate over the mechanisms governing magnetic field detection (Kalmijn, 1982, 1984; Hodson, 2000; Molteno and Kennedy, 2009). However, the most current explanation of elasmobranch magnetic field detection is through the process of indirect-based magnetoreception (Kalmijn, 1973, 1982). In the active mode for this mechanism, movement through magnetic fields induces electrical currents around the bodies of moving aquatic organisms, including elasmobranchs. This induced voltage is presumed to be detected by an elasmobranch's numerous cephalic ampullary pores, which consequently may give the respective organism relative geolocation information (Kalmijn, 1982, 1984).

Exploiting an elasmobranch's ability to detect magnetic fields, research demonstrates that supernormal magnetic stimuli, such as those produced by permanent magnets, can elicit repellent responses in elasmobranchs (Stoner and Kaimmer, 2008; Rigg et al., 2009; Robbins et al., 2011; O'Connell et al., 2010, 2011a, 2012a, 2013a,b). Scientists hypothesize that these responses occur due to flux differentials that exist between permanent magnets and geomagnetic fields. For example, grade C8 barium-ferrite permanent magnets generate an approximate surface magnetic flux of 3850 G, where the geomagnetic flux ranges from 0.25 to 0.65 G. Being several orders of magnitude greater in strength, the novel stimulus produced by the permanent magnets is hypothesized to overstimulate the ampullary system and deter approaching elasmobranchs. To date, numerous studies tested this hypothesis and have produced mixed findings (Stoner and Kaimmer, 2008; Rigg et al., 2009; Robbins et al., 2011; O'Connell et al., 2010, 2011a, 2012b, 2013a). Stoner and Kaimmer (2008) examined the behavior of Pacific halibut (*Hippoglossus stenolepis*), a teleost, and spiny dogfish (*Squalus acanthias*), an elasmobranch, in response to neodymium-iron-boride magnets ($Nd_2Fe_{14}B$). *H. stenolepis* showed no behavioral modification in the presence of magnets, whereas *S. acanthias* exhibited signs of irritation. Similarly, Rigg et al. (2009) conducted a behavioral assessment on the effect of ceramic magnets on several elasmobranchs and one teleost species, the seabass (*Lates calcarifer*). No behavioral effect on *L. calcarifer* was observed; however, elasmobranchs exhibited deterrent responses. Furthermore, inter-specific variations in deterrent responses were suggested to be a consequence of differing feeding ecologies. Robbins et al. (2011) conducted a study examining the potential utility of permanent magnets on the Galapagos shark (*Carcharhinus galapagensis*). The results from this study demonstrated that magnetic field orientation governed repellency success with success being inversely correlated with conspecific density. Besides basic behavioral analyses, several studies were conducted which used permanent magnets for conservation applications to determine their potential to reduce elasmobranch capture in fisheries and beach nets (O'Connell et al., 2011a,b, 2012a,b, 2013b). These studies demonstrated that magnetic deterrent responses were species-specific and also were highly correlated with variations in environmental and biological parameters.

With mixed findings pertaining to the utilization of magnets in longline and hook-and-line-related studies (O'Connell et al., 2011b, 2012b), magnetic repellent research has recently focused on beach net applications. Beach nets are devices utilized in areas such as South Africa (Dudley, 1997) and Australia (Hamer, 1993; Anon, 1998) to minimize the potentially dangerous interactions between large sharks and beachgoers. However, although beach nets are successful at reducing this conflict, substantial and localized elasmobranch mortality occurs (Dudley, 1997; Dudley and Cliff, 1993; Dudley and Gribble, 1999) in addition to non-target species mortality (Gribble et al., 1998). To address this mortality and using the findings from previous beach net-associated magnetic repellent analyses (O'Connell et al., 2012a, 2013a,b), an eco-friendly conservation technology, known as the Sharksafe barrier, was developed (O'Connell et al., 2014). This barrier contains two key stimuli: (1) grade C8 barium-ferrite ($BaFe_{12}O_{19}$) permanent magnets and (2) visual stimuli—PVC piping. Using this technology, a previous study demonstrated that swimming patterns of all interacting *Carcharodon carcharias* significantly changed in the presence of the barrier and that the barrier can withstand heavy seas (exceeding 4 m), is cost-effective, does not require electrical input, and requires little maintenance since barium-ferrite magnets do not degrade in seawater. However, this experiment (O'Connell et al., 2014) only evaluated changes in shark swim patterns, not whether the technology could be used to exclude sharks which is integral to understanding the utility of this technology as an alternative to beach nets. Furthermore, observations could not be conducted in low visibility conditions (e.g. high turbidity and nighttime) due to safety concerns and difficulties in making accurate behavioral observations.

In the present Sharksafe barrier study, there were two key objectives: (1) to determine if the Sharksafe barrier can exclude bull sharks (*Carcharhinus leucas*) from bait, and (2) to determine if the swimming behavior of *C. leucas* varies based on visibility parameters (e.g. high vs. low light intensity). We hypothesized that permanent magnetic barrier regions (i.e. regions containing PVC pipes and magnets) would result in significant behavioral exclusion in comparison to procedural control (i.e. regions containing PVC pipes and no magnets) and control (i.e. no PVC pipes and no magnets) regions. Secondly, since context-specific variations in sensory modalities may be directly linked to light intensity characteristics and concurrently may alter behavior (O'Connell et al., 2013a), it was hypothesized that light intensity variations would significantly alter the barrier's exclusion capabilities and *C. leucas* behavior. Thirdly, due to varying levels of conspecifics and heterospecifics, it was hypothesized that situations arising from increased intra- and inter-specific competition (e.g. Robbins et al., 2011; O'Connell et al., 2013b) may result in significant reductions in the exclusion capabilities of the Sharksafe barrier on interacting *C. leucas*.
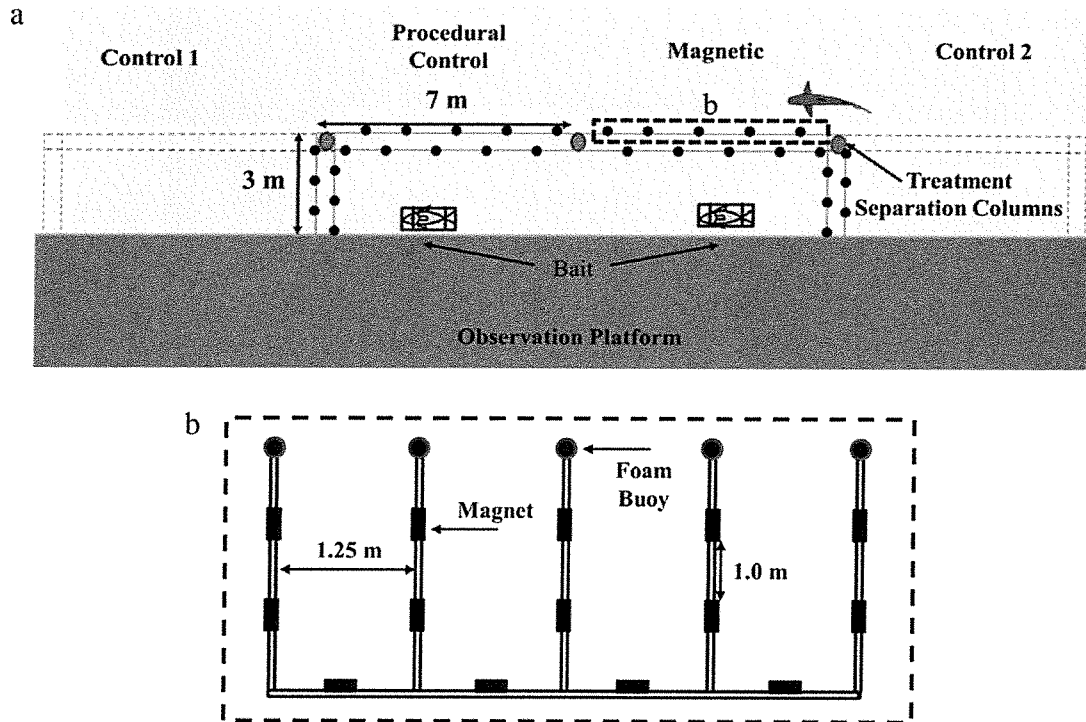
Fig. 1. Experimental setup. (a) Top view. The barrier was composed of four equal-sized (7 × 3 m) regions, two controls—unmanipulated areas, one procedural control, and one magnetic region. Both the procedural control and magnetic regions consisted of two rows of treatment columns; each containing five vertical columns (black dots) at 1.25 m apart. The columns were made of 38.1 mm diameter PVC tubing. The magnetic columns contained two 152 × 102 × 12.7 mm grade C8 $BaFe_{12}O_{19}$ permanent magnets (1 m apart) that were covered in black duct tape. The procedural control columns contained two visually identical sham magnets, or two similar regions covered in black duct tape. Between adjacent pipes and attached to the PVC frame on the seafloor, was either a permanent magnet or a sham magnet. Between treatment regions, one, 25.4 mm diameter PVC pipe and a foam buoy were placed to serve as a treatment separation column. (b) Side profile of one row of the magnetic region.

2. Methods

The study was conducted in Bimini, Bahamas during the month of February 2014. Over the course of 18 days, a total of 114, 30-min trials were conducted, irrespective of tide and during periods characterized as having high (e.g. light intensity ≥ 1 lux) and low (e.g. light intensity <1 lux) light intensities. The designated study site was located adjacent to a concrete platform and consisted of a sandy substrate that was approximately 3 m in depth. Throughout the experiment, HD GoPro Hero 3 1080p cameras were deployed to determine the quantity of individual *C. leucas* that interacted with the barrier. Post hoc video analysis permitted researchers to identify unique characteristics that were often specific to individual sharks, such as: size, sex, presence/absence of a tag, color, presence/absence of fin damage, and presence/absence of scars. However, since poor water visibility conditions sometimes restricted post hoc video analysis capabilities, videos were used solely for shark identification and not for assessing shark behavior around the barrier. Furthermore, these unique identification characteristics were also employed to identify non-target species, such as lemon sharks (*Negaprion brevirostris*), nurse sharks (*Ginglymostoma cirratum*), yellow stingrays (*Urobatis jamaicensis*), and great barracuda (*Sphyraena barracuda*). This research was conducted under conditions of the assigned Bahamas Department of Marine Resources permit (MAF/FIS/17).

2.1. Barrier experiment

The barrier frame consisted of 38.1 mm diameter polyvinyl chloride (PVC) piping. To properly deploy the barrier, two, 14 m (L) × 3 m (W) PVC frames were constructed. At 1.25 m intervals on each PVC frame, screw eyes were placed to permit the attachment of the treatment columns. Treatment columns consisted of 3 m (length)× 38.1 mm diameter PVC piping with attached 0.01 m^2 foam buoys to ensure that each pipe was suspended vertically in the water column (Fig. 1).

The first PVC frame contained two treatment regions: (1) procedural control and (2) magnetic. Both regions consisted of eight, 38.1-mm diameter treatment columns. The procedural control columns contained two sham magnets, which were two, 152.0-mm regions covered in black duct tape that were separated by 1 m. At identical locations, the magnetic columns contained similarly sized 152 × 102 × 12.7 mm grade C8 $BaFe_{12}O_{19}$ permanent magnets. Magnets were covered in black duct tape to make them visually identical to the sham magnets. Between each pipe, attached to the PVC frame, and dependent on

the treatment region was either a permanent magnet ($152 \times 102 \times 51$ mm) or a clay brick sham magnet ($152 \times 102 \times 67$ mm). Additionally, between each treatment region, one, 25.4 mm diameter PVC pipe with an attached foam float was placed to serve as a treatment separation column and to standardize the location of recordable behaviors associated with each treatment region. Halfway through the experiment, the positioning of the procedural control and magnetic barrier regions were switched to reduce the possibility of side preference-based behaviors.

The second PVC frame was identical in construction to the first PVC frame; however, neither magnets nor sham magnets were added to the columns. The second PVC frame was placed 0.5 m behind the first frame and was positioned so that the PVC columns alternated with the treatment columns in the first row (Fig. 1). These frames were placed flush against the substrate with the terminal portions placed flush against the concrete dock to create a rectangular experimental region with the dimensions of 14 m $\times$ 3 m. Lastly, to complete the experimental design, two equal-sized control regions (7 m $\times$ 3 m) were established on either side of the main barrier. These control regions were unmanipulated areas.

Prior to the experiment, fluorescein dye tabs were placed within each experimental region to assess if current flow would evenly disburse olfactory stimuli around and outside the barrier. Once assessed, every 30 min trial, one chum bag was placed within each experimental region. These chum bags were filled with approximately 1.81 kg of bait, which consisted of *S. barracuda*, wahoo (*Acanthocybium solandri*), greater amberjack (*Seriola dumerili*), longfin yellowtail (*Seriola rivoliana*), and/or Tournament Master Chum® menhaden blocks. Each bag contained equal quantities of each bait type to alleviate the possibility of preference-based behaviors. Prior to conducting a trial, one control region was randomly selected for behavioral observations. Throughout each 30-min trial, *C. leucas* behavioral interactions and the interactions of other non-target species were recorded by one researcher who stood on the adjacent concrete dock. The behaviors recorded were: (1) visits—fish swimming within one body length of the barrier, (2) avoidances—a visit followed by an abrupt change in behavior such as an acceleration away or a 45°, 90°, or 180° turn away from the barrier, (3) entrances—a visit and a pass through a particular treatment region, and (4) pass arounds—a visit followed by a fish swimming adjacent to an entire experimental region, but not avoiding or passing through the area. Each behavior was aggregated for each species and for each trial. Also, during each behavioral interaction towards the barrier, shark quantity (heterospecifics and conspecifics) was recorded using topside observation techniques.

Light intensity and water temperature were measured by placing two HOBO Pendant Temperature/Light data loggers (64K-UA-002-64) in the water, one at the sea surface and one on the seafloor. Salinity was measured using a portable refractometer (Model: RHS-10ATC).

2.1.1. Bull shark statistical analysis

Data collected throughout the experiment was in the form of frequencies (i.e. counts) for *C. leucas*. However, this data was multi-dimensional, where the main effects of several variables and interaction terms between these variables were of interest. Therefore, the traditional Chi-square analysis was inefficient in testing hypotheses that involve the multi-dimensions, and instead, we applied a Poisson generalized linear mixed effect model to data in each category: avoidance, entrance and pass-around, respectively. The multinomial distribution is the joint distribution of Poisson distributions, conditional upon their total sum (Dobson and Barnett, 2008). Furthermore, treatment positioning was not randomized on a per-trial basis, and thus *C. leucas* behaviors were not considered independent since multiple interactions from one individual shark may have occurred within a trial. This may violate the assumption in generalized linear models that data are independent. Thus we treated trial as a random effect, because data were not independent whereas we treated the other variables as fixed effects.

Mathematical form of our generalized linear mixed effect model is:

$$Y = X\beta + R + \varepsilon \tag{1}$$

Y represents the column vector of the response variable (counts of shark responses), X is the design matrix of explanatory variables, including all possible interaction terms, β is the column vector of coefficients that correspond to explanatory variables, R is the vector of individual trials, which is a random effect, and ε represents the vector of errors, which are assumed to follow a normal (Gaussian) distribution whose mean is zero and whose variance is constant. The fixed effects (i.e., X) were treatment type (discrete), water visibility (continuous), heterospecific density (continuous), and conspecific density (continuous).

The mixed effect model (Eq. (1)) was implemented using the 'lme4' package of R (Bates et al., 2012; Hyun et al., 2014; R 3.3.0 Statistical Program). Forward selection was used to determine the best fit model for the data, starting with a null model, of which subsequent models were created by adding one or several explanatory variables to determine their effect on the response variables (i.e. avoidance frequency, entrance frequency, and pass around frequency). We tested the contribution of an explanatory variable, examining the difference in the log-likelihood (Hyun et al., 2014; Faraway, 2006):

$$-2 \cdot \Delta\ell \sim \chi^2_{\Delta par} \tag{2}$$

$\Delta\ell$ is the difference in the log-likelihood between nested and non-nested models in the forward selection process (Table 1), and Δpar is the difference in the number of free parameters between two models. Model selection criteria included: Akaike Information Criteria (AIC), and behavior of model residuals using a quantile–quantile (Q–Q) plot, and associated P-values (Table 1). Lastly, no entrances were observed in relation to the procedural control and magnet regions, whereas a substantial

Table 1

Results from the mixed effect models pertaining to bull shark (*Carcharchinus leucas*) behavior. For entrance frequency, data were transformed to "total entrances + 1" for each treatment region to improve the interpretability of the data, as no entrances occurred through the procedural control or magnet treatment regions throughout the entire experiment. Trial (R) is treated as a random effect and the others are treated as fixed effects. These fixed variables were T (treatment), Con (conspecific density), Het (heterospecific density), Upper (sea surface light intensity), and Lower (seafloor light intensity). Selected models for avoidance, entrance, and pass around frequencies were A13, B7, and C2 respectively, based on a combination of Akaike Information Criteria (AIC), and behavior of the residuals of a model using a quantile–quantile (Q–Q) plot, and associated P-values. Significant models for main effects ($P \leq 0.05$) and interaction terms ($P \leq 0.1$) are in bold.

Model	Log likelihood	$-2(\Delta l)$	ΔPAR	P-value	AIC
Avoidance Frequency					
1 + R	−456.60	–	–	–	917.21
1+R+T	**−382.05**	**1295.26**	**2**	**<0.001**	**772.10**
1 + R + Con	−456.49	1369.69	1	0.63	918.98
1 + R + Het	−455.69	1368.90	1	0.18	917.39
1 + R + Upper	−456.48	1369.69	1	0.62	918.97
1 + R + Lower	−456.22	1369.43	1	0.38	918.44
1 + R + T + Con	−381.15	1145.25	1	0.18	772.30
1 + R + T + Het	−381.97	1146.07	1	0.68	773.93
1 + R + T + Upper	−381.89	1145.99	1	0.57	773.78
1 + R + T + Lower	−381.47	1145.58	1	0.28	772.94
1 + R + T + Con + T * Con	**−375.30**	**1137.60**	**2**	**0.003**	**764.61**
1 + R + T + Het + T * Het	**−379.45**	**1143.38**	**2**	**0.08**	**772.90**
1 + R + T + Upper + T * Upper	**−374.63**	**1138.41**	**2**	**<0.001**	**763.25**
1 + R + T + Lower + T * Lower	**−373.85**	**1136.79**	**2**	**0.002**	**763.70**
Entrance Frequency					
1 + R	−1602.84	–	–	–	3209.70
1 + R + T	**−289.65**	**3495.32**	**2**	**<0.001**	**587.30**
1 + R + Con	−1602.84	4808.00	1	0.31	3210.70
1 + R + Het	**−1598.22**	**4803.89**	**1**	**0.002**	**3202.40**
1 + R + Upper	−1601.42	4807.09	1	0.09	3208.80
1 + R + Lower	−1601.83	4807.50	1	0.16	3209.70
1 + R + T + Con	**−284.26**	**863.56**	**1**	**0.001**	**578.53**
1 + R + T + Het	−288.77	868.06	1	0.19	587.54
1 + R + T + Upper	−289.16	868.45	1	0.32	588.31
1 + R + T + Lower	−289.03	868.32	1	0.27	588.06
1 + R + T + Con + T * Con	−283.80	852.33	2	0.63	581.61
1 + R + T + Het + T * Het	−288.39	865.93	2	0.68	590.78
1 + R + T + Upper + T * Upper	−288.25	866.56	2	0.40	590.49
1 + R + T + Lower + T * Lower	−288.12	866.18	2	0.61	592.24
Pass Around Frequency					
1 + R	−1250.54	–	–	–	2505.10
1 + R + T	**−760.15**	**3261.22**	**2**	**<0.001**	**1528.30**
1 + R + *Con*	−1250.52	3751.59	1	0.87	2507.00
1 + R + Het	−1249.47	3750.54	1	0.14	2504.90
1 + R + Upper	−1250.53	3751.59	1	0.92	2507.10
1 + R + Lower	−1250.50	3751.57	1	0.81	2507.00
1 + R + T + Con	−760.06	2280.36	1	0.68	1530.10
1 + R + T + Het	−759.62	2279.92	1	0.31	1529.20
1 + R + T + Upper	−759.78	2280.08	1	0.39	1529.60
1 + R + T + Lower	−760.05	2280.35	1	0.67	1530.10
1 + R + T + Con + T * Con	**−757.39**	**2277.52**	**2**	**0.07**	**1528.80**
1 + R + T + Het + T * Het	−758.81	2278.05	2	0.44	1531.60
1 + R + T + Upper + T * Upper	−759.73	2279.29	2	0.94	1533.50
1 + T + Lower + T * Lower	−759.51	2279.62	2	0.78	1535.00

Abbreviations: 1 = y-axis intercept, Δl = change in log likelihood value between former model and model being considered, ΔPAR = change in degrees of freedom between former model and model being considered, P-value = the level of significance of the explanatory variable added, AIC = Akaike Information Criterion (2 * (log likelihood) + 2 * number of parameters), a model selection criterion.

quantity of entrances was observed towards the control region. Therefore, entrance data were transformed by adding one behavioral count to each treatment region (i.e. one entrance towards the control, procedural control, and magnet region).

2.1.2. Non-target species statistical analysis

Similar to *C. leucas* behaviors; visits, avoidances, entrances, and pass arounds were recorded for all other interacting species that could be identified from surface observations. Data were then aggregated by species and trial. These data were transformed into frequencies pertaining to each behavior type (e.g. avoidance frequency = total trial avoidances per total trial visits). However, interactions associated with these additional species were infrequent and thus GLMMs were not appropriate. Therefore, using R 2.13.0 Statistical Program (www.r-project.org), Kruskal–Wallis tests were employed to assess if any significant variation existed in behavioral frequencies with treatment type. If significant variation was
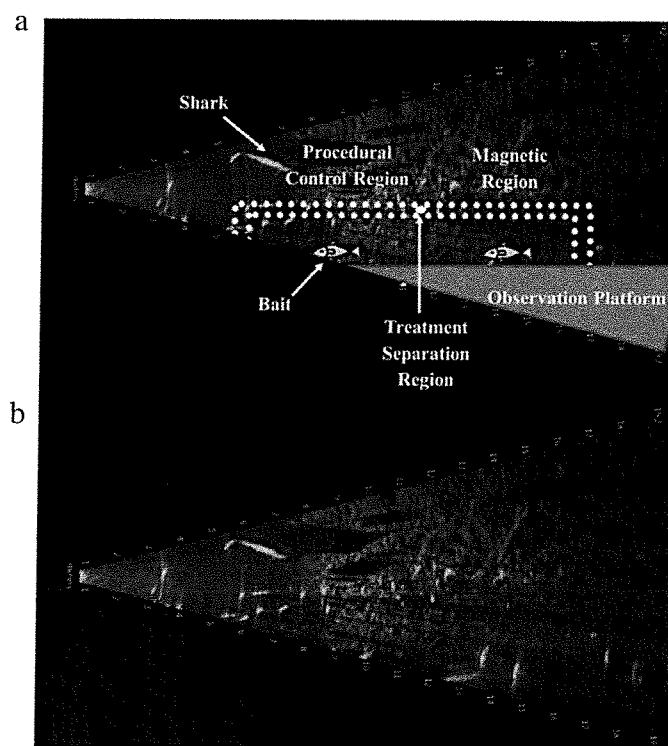
Fig. 2. Example of one video frame that was captured from ARIS video output. (a) A labeled frame. Note, the white dots associated with treatment regions do not correlate with the exact positioning and quantity of pipes used to create the structure. (b) An unlabeled version of the same frame.

detected, post hoc Wilcoxon rank sum tests with Bonferroni correction were performed on each possible treatment type pair (e.g. control vs. procedural control) to determine if one treatment type was solely responsible for behavioral significance.

2.2. Adaptive Resolution Imaging Sonar (ARIS)

For each trial, an ARIS Explorer 3000 dual-frequency acoustic camera (SoundMetrics, Seattle, WA) was deployed. This camera emits 128 acoustic beams (0.2° beam width) and operates at both 1.8 and 3.0 MHz to form an image based on the acoustic returns of a target object regardless of the ambient light conditions (e.g. day vs. night and/or high vs. low turbidity). This camera was placed on an adjacent dock to capture shark behavioral interactions around both the procedural control and magnetic regions (Fig. 2). The camera settings were adjusted so that the maximum recording range was activated. Imaging data were recorded in a computer hard disk and appropriately labeled to permit accurate post hoc analysis.

2.2.1. ARIS vs. field observation techniques

Since this is the first study to employ the ARIS technology, it is essential to determine if the technology could be used for future shark behavioral experiments. Therefore, to assess the utility of the technology and to determine the relationship between the behavioral observations associated with ARIS footage and field observations, post hoc video analyses were conducted. Three trained volunteers analyzed the same twelve, 30-min trials. These trials consisted of three high light intensity trials (i.e. light intensity ≥ 1 lux) and three low light intensity trials (i.e. light intensity < 1 lux). Volunteers recorded C. leucas avoidance, entrance, and pass around behaviors towards both procedural control and magnetic regions of the exclusion barrier; however, volunteers were only told where experimental regions commenced and terminated and were unaware of designated treatment regions until behavioral quantification was completed. Data from each volunteer were then calculated for per-trial frequencies for each behavior type (e.g. total avoidances per total visits). Furthermore, since data were not normally distributed and to determine if there was a significant difference between volunteer and field observation per trial frequencies, Kruskal–Wallis tests were employed for each behavior type and for each treatment region (e.g. procedural control and magnetic).

2.2.2. ARIS distance

As each C. leucas was observed to swim adjacent to both treatment regions, the shortest distance between a shark's head and the treatment columns was calculated using the ARIS post hoc analysis software (ARIScope V1.3.0). Distance

measurements were obtained when a shark initially approached and just prior to the shark leaving a treatment region. These distances were averaged and the resultant value was used for statistical analyses pertaining to that interaction. Interactions which only occurred towards one treatment region were discarded from analysis. To determine if there was a difference between shark distance relative to treatment regions, data were subjected to a paired t-test. It is important to note that due to the ARIS capture angle (30° horizontal), the field of view is greater with distance from the camera. For example, behaviors could only be recorded at a maximum distance of 2.5 m from the treatment region closest to the camera, whereas behaviors could be recorded at a distance of 3.5 m from the furthest region. Therefore, during video analysis, only behaviors occurring within 2.5 m from treatment regions were used for analysis. This standardized the location for distance calculations between treatment regions.

In addition to treatment regions, calculations regarding shark distance from the barrier were made in relation to light intensity. All distance calculations were rearranged into high (e.g. mean trial light intensity ≥ 1 lux) vs. low (e.g. mean trial light intensity < 1 lux) light intensity categories, regardless of treatment type. To determine if shark distance from the barrier differed relative to the light intensity categories, data were subjected to an unpaired t-test.

2.2.3. ARIS speed

As each C. leucas was observed to swim adjacent to both treatment sections, swim speed was calculated using the ARIS post hoc analysis software. From the software, the x, y coordinates were obtained from each shark as it initially approached and just prior to leaving a treatment region, and the straight line distance traveled was calculated using the Euclidean distance formula. With the time interval between two points, swim speed was calculated. Interactions which only occurred towards one treatment region during the trial were discarded from this analysis. To determine if shark swim speed differed relative to each treatment region, data were subjected to a paired t-test.

In addition to treatment regions, swim speeds were rearranged into high (e.g. mean trial light intensity ≥ 1 lux) vs. low (e.g. mean trial light intensity < 1 lux) light intensity categories, regardless of treatment type. To determine if shark swim speed differed relative to the light intensity categories, an unpaired t-test was used.

3. Results

A total of 114, 30-min trials were conducted over the course of eighteen days. During this period, a minimum of twenty-three different C. leucas were identified using short-term identification characteristics through post hoc video analysis. Using the ARIS post hoc analysis software, sharks ranged from 1.6 to 2.8 m in total length. Throughout the experiment, sea surface temperature was 26.44° C $\pm$ 0.92 (mean $\pm$ standard deviation), salinity was 36.70 ppt $\pm$ 1.20, sea surface light intensity ranged from <0.01 to 23,422.40 lux, seafloor light intensity ranged from <0.01 to 5260.30 lux, conspecific density ranged from 1 to 11 and heterospecific density ranged from 1 to 4.

3.1. Bull shark behavior

3.1.1. Avoidance frequency

For avoidance frequency, the best fit model (A13) included the main effects of treatment type (T), sea surface light intensity (Upper), and the interaction between T and Upper (T*Upper). This model outperformed all other models and contained an AIC of 763.25 (Table 1). The coefficient and associated P-value with the selected model demonstrate that the influence of the magnetic region ($P < 0.001$), procedural control region ($P < 0.001$) and sea surface light intensity ($P = 0.01$) had a significantly positive relationship with C. leucas avoidance frequency (Table 2). Based on model coefficients, the magnetic region resulted in a greater frequency of avoidances than the procedural control region, and increases in sea surface light intensity resulted in an overall increase in avoidance frequency. In addition, the interaction between the procedural control and magnetic regions with sea surface light intensity had a significantly negative relationship with avoidance frequency ($P = 0.004$; $P = 0.06$, respectively), indicating that increases in light intensity in either treatment region yielded a decrease in avoidance frequency (Table 2; Fig. 3a).

3.1.2. Entrance frequency

Data pertaining to entrance frequency exhibited a clear behavioral distinction between treatment types (Control = 1260, Procedural Control and Magnet = 0). For secondary validation, an applied mixed effect model to the transformed data (i.e. adding one behavioral count to each treatment type) for entrance frequency revealed that the best fit model (B7) included the main effects of T and Con. Model B7 outperformed all other models and had the lowest AIC of 578.5 (Table 1) with a significant reduction in entrance frequency towards the magnetic ($P < 0.001$) and procedural control ($P < 0.001$) regions, and a significant increase in entrance frequency with increases in Con ($P < 0.001$) (Table 2; Fig. 3b).

3.1.3. Pass around frequency

For pass around frequency, the best fit model (C2) included the main effect of T. Model C2 outperformed all other models and contained an AIC of 1528.30 (Table 1), with the magnetic ($P < 0.001$) and procedural control ($P < 0.001$) regions

Table 2

Coefficients, standard errors, t statistic and P-values of explanatory variables for best models A13, B7, C2 for avoidance, entrance, and pass around frequencies, respectively, for the bull shark (*Carcharhinus leucas*) in relation to the barrier treatment regions. For entrance frequency, data were transformed to "total entrances + 1" for each treatment region to improve the interpretability of the data, as no entrances occurred through the procedural control and magnet region throughout the entire experiment. Significant models for main effects ($P \leq 0.05$) and interaction terms ($P \leq 0.1$) are in bold.

| Explanatory variable	Coefficient	Standard error	t	P-value
Avoidance frequency				
Intercept	−5.51	0.58	−9.47	<0.001
Magnet	3.39	0.59	−5.76	<0.001
Procedural control	2.40	0.61	3.94	<0.001
Upper	1.59	0.62	2.58	0.01
Magnet: Upper	−1.81	0.63	−2.87	0.004
P. control: Upper	−1.22	0.65	−1.86	0.06
Entrance frequency				
Intercept	−0.52	0.06	−8.78	<0.001
Magnet	−7.07	1.00	−7.07	<0.001
P. control	−7.09	1.00	−7.09	<0.001
Conspecifics	0.04	0.01	3.33	<0.001
Pass around frequency				
Intercept	−1.97	0.06	−31.20	<0.001
Magnet	1.65	0.07	23.68	<0.001
P. control	1.69	0.07	24.44	<0.001
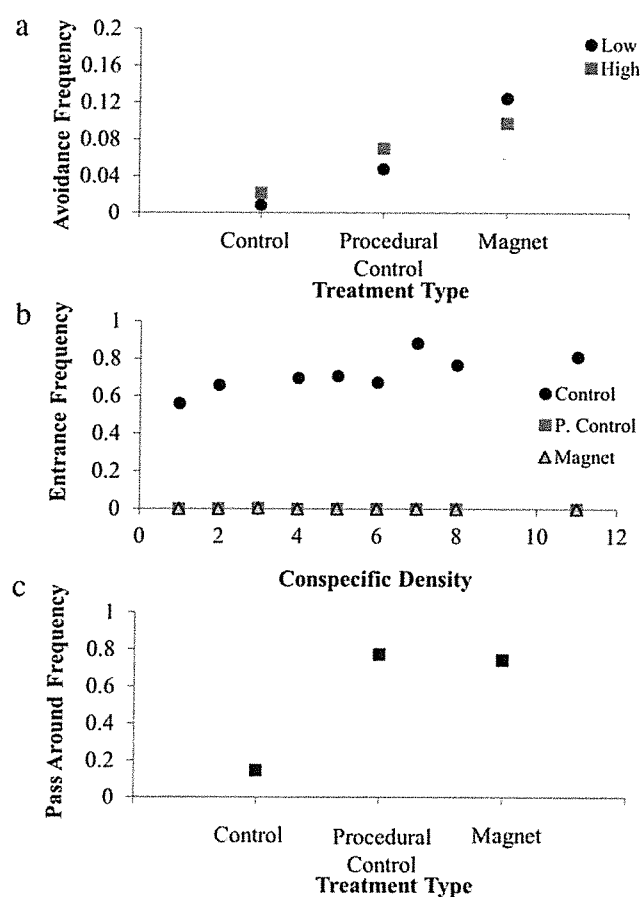
Fig. 3. Graphical representations for the best fit models for each bull shark (*Carcharhinus leucas*) behavior (total quantity of behavior per total visits). (a) Best fit model, A13, pertaining to the outcome variable, avoidance frequency and significant predictor variables, treatment type (T), sea surface light intensity (Upper), and the interaction between the two (T*Upper). Sea surface light intensity was separated into mean per trial low (< 1 lux) and high (≥ 1 lux) light intensities. (b) Best fit model, B7, pertaining to the outcome variable, entrance frequency and significant predictor variables, T and conspecific density. (Con) For entrance frequency and since no entrances were observed towards the procedural control and magnet treatment region, all data were transformed to (total avoidances+1)/total visits for each treatment region to improve the interpretability of the data. (c) Best fit model, C2, pertaining to the outcome variable, pass around frequency and significant predictor variable, T.

Table 3

Elasmobranch and great barracuda (*Sphyraena barracuda*) behavior towards the barrier apparatus that contained three treatment areas (control, procedural control and magnetic). Quantity (n) indicates the sample size for each species. H and *P*-values are the associated test statistics obtained from the Kruskal–Wallis tests. Significant findings ($P \leq 0.05$) are in bold.

Species	Quantity (n)	Behavior	H	P-value
Nurse shark (*Ginglymostoma cirratum*)	9	Avoidance	3.98	0.14
		Entrance	**15.36**	**<0.01**
		Pass around	0.98	0.61
Yellow stingray (*Urobatis jamaicensis*)	8	Avoidance	N/A	N/A
		Entrance	0.52	0.77
		Pass around	N/A	N/A
Lemon shark (*Negaprion brevirostris*)	5	Avoidance	1.17	0.56
		Entrance	**7.62**	**0.02**
		Pass around	**6.06**	**0.05**
Great barracuda (*Sphyraena barracuda*)	6	Avoidance	N/A	N/A
		Entrance	0.44	0.80
		Pass around	1.86	0.40

Table 4

Results from the post hoc Wilcoxon rank sum tests demonstrating which individual treatment type pairings were responsible for behavioral significance for the nurse (*Ginglymostoma cirratum*) and lemon (*Negaprion brevirostris*) sharks. Significant findings ($P \leq 0.05$) are in bold.

Species	Procedural control	Magnetic
Nurse shark (*Ginglymostoma cirratum*)		
Entrance rate		
Control	$Z = 2.29, P = 0.13$	$Z = 15.17, P < 0.001$
Procedural control	–	$Z = 5.31. P = 0.02$
Lemon shark (*Negaprion brevirostris*)		
Entrance rate		
Control	$Z = 4.36, P = 0.04$	$Z = 4.36. P = 0.04$
Procedural control	–	UNDEFINED
Pass around rate		
Control	$Z = 3.97, P = 0.05$	$Z = 4.09. P = 0.04$
Procedural control	–	$Z = 1.23, P = 0.27$

yielding a significant increase in pass around frequency (Table 2; Fig. 3c). Although not associated with the best fit model, the interaction between T and Con (T*Con; $P = 0.07$) had a significant influence on pass around frequency.

3.1.4. Predation attempts

Throughout the experiment, there were eight *C. leucas* predation attempts on the Atlantic tarpon (*Megalops atlanticus*) which occurred within the experimental region. Although too infrequent for statistical analysis, these attempts seemed to follow a consistent pattern. To initiate the predation attempt, *C. leucas* exhibited an increase in tail-beat frequency and a directed acceleration towards *M. atlanticus*. In response, *M. atlanticus* either swam directly parallel to the barrier (3 occasions) or through the barrier (5 occasions). On the occasions where *M. atlanticus* swam through the barrier, *C. leucas* continued pursuit until the outer row of barrier columns, and made an immediate ±180° turn and accelerated away from the barrier. When swimming parallel to the barrier, *C. leucas* continued pursuit of *M. atlanticus* until outside the range of visibility.

3.2. Non-target species behavior

Throughout the experiment, four non-target species were observed that were of sufficient quantity for analysis: nurse shark (*Ginglymostoma cirratum*: $n = 9$; size range $= 1.84 \pm 0.52$ m in total length), yellow stingray (*Urobatis jamaicensis*; $n = 8$; size range $= 0.40 \pm 0.09$ m in disc width), lemon shark (*Negaprion brevirostris*: $n = 5$; size range $= 1.96 \pm 0.32$ m in total length), and great barracuda (*Sphyraena barracuda*; $n = 6$; size range $= 1.10 \pm 0.20$ m in total length). Results from Kruskal–Wallis tests illustrate that avoidance frequency for all species did not significantly differ with treatment type; however, entrance frequency of *G. cirratum* and *N. brevirostris*, and pass around frequency of *N. brevirostris* did significantly differ with treatment type (Table 3).

For *G. cirratum*, post hoc Wilcoxon rank sum tests with Bonferroni correction indicated that the difference in entrance frequency was significant between control (C)–magnetic (M) and procedural control (PC)–M treatment pairings (Table 4). For *N. brevirostris*, post hoc Wilcoxon rank sum tests with Bonferroni correction indicated that differences in entrance and pass around frequencies were significant between C–PC and C–M treatment pairings; however, since no entrances occurred through the PC or M regions this treatment pairing was undefined (Table 4).

Table 5
Results from a Kruskal–Wallis test illustrating the variation between field observations and post hoc ARIS camera observations of bull shark (*Carcharhinus leucas*) behavior around the procedural control (PC) and magnetic (M) regions of the barrier. The same observer that made the field observations also participated in the post hoc ARIS camera observations. Furthermore, two additional trained volunteers participated in the post hoc video analysis. A total of twelve trials (6 h) were used for this analysis. H and *P*-values are the associated test statistic obtained from the Kruskal–Wallis tests. Significant findings ($P \leq 0.05$) are in bold.

H	*P*-value
Avoidance PC	
1.64	0.65
Entrance PC	
Undefined	*Undefined*
Pass around PC	
3.84	0.28
Avoidance M	
1.30	0.73
Entrance M	
Undefined	*Undefined*
Pass around M	
1.81	0.61
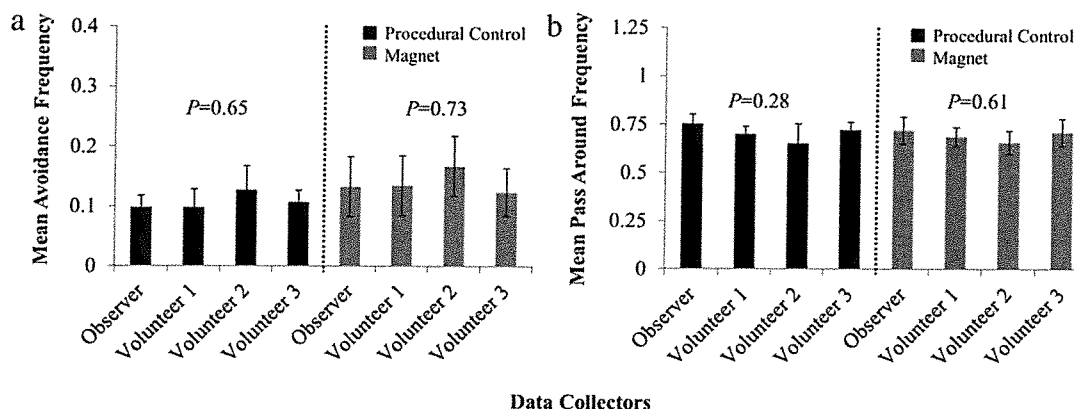
Fig. 4. ARIS accuracy experiment. (a) Mean avoidance frequencies of bull sharks (*Carcharhinus leucas*) towards the procedural control (black bars) and magnet regions (gray bars), obtained from actual field observations (Observer) and from three volunteers who participated in post hoc video analysis (Volunteers 1–3). (b) Mean pass around frequencies of *C. leucas* towards the procedural control and magnet regions obtained from actual field observations (Observer) and from post hoc video analysis (Volunteers 1–3).

3.3. Behavioral observations using ARIS

3.3.1. ARIS vs. field observation techniques

Procedural control region. The mean avoidance frequencies (±SD) which occurred towards the procedural control region were: fieldobserver(O) = 0.09 ± 0.08, volunteer 1(V1) = 0.09 ± 0.08, volunteer 2(V2) = 0.12 ± 0.14, and volunteer 3(V3) = 0.11 ± 0.08. The mean pass around frequencies (±SD) for the procedural control region were: O = 0.75 ± 0.16, V1 = 0.70 ± 0.15, V2 = 0.65 ± 0.67, and V3 = 0.72 ± 0.13. Since no entrances occurred during field and volunteer observations, mean values were not calculated. Kruskal–Wallis tests demonstrate that avoidance (H = 1.64, d.f. = 3, $P = 0.65$), entrance (H = undefined, d.f. = 3, P = undefined), and pass around (H = 3.84, d.f. = 3, $P = 0.28$) frequencies associated with the procedural control region did not significantly differ between field observation and post hoc analysis of ARIS data (Table 5; Fig. 4).

Magnetic region. The mean avoidance frequencies ±(SD) towards the magnetic region were: O = 0.13 ± 0.16, V1 = 0.13 ± 0.16, V2 = 0.17 ± 0.17, and V3 = 0.12 ± 0.12. The mean pass around frequencies ±(SD) for the magnetic region were: O = 0.72 ± 0.23, V1 = 0.69 ± 0.19, V2 = 0.66 ± 0.21, and V3 = 0.71 ± 0.23. Since no entrances occurred during field and volunteer observations, mean values were not calculated. Kruskal–Wallis tests demonstrate that avoidance (H = 1.30, d.f. = 3, $P = 0.73$), entrance (H = undefined, d.f. = 3, P = undefined), and pass around (H = 1.81, d.f. = 3, $P = 0.61$) frequencies associated with the magnetic region did not significantly differ between field observation and post hoc analysis of ARIS video (Table 5; Fig. 4).
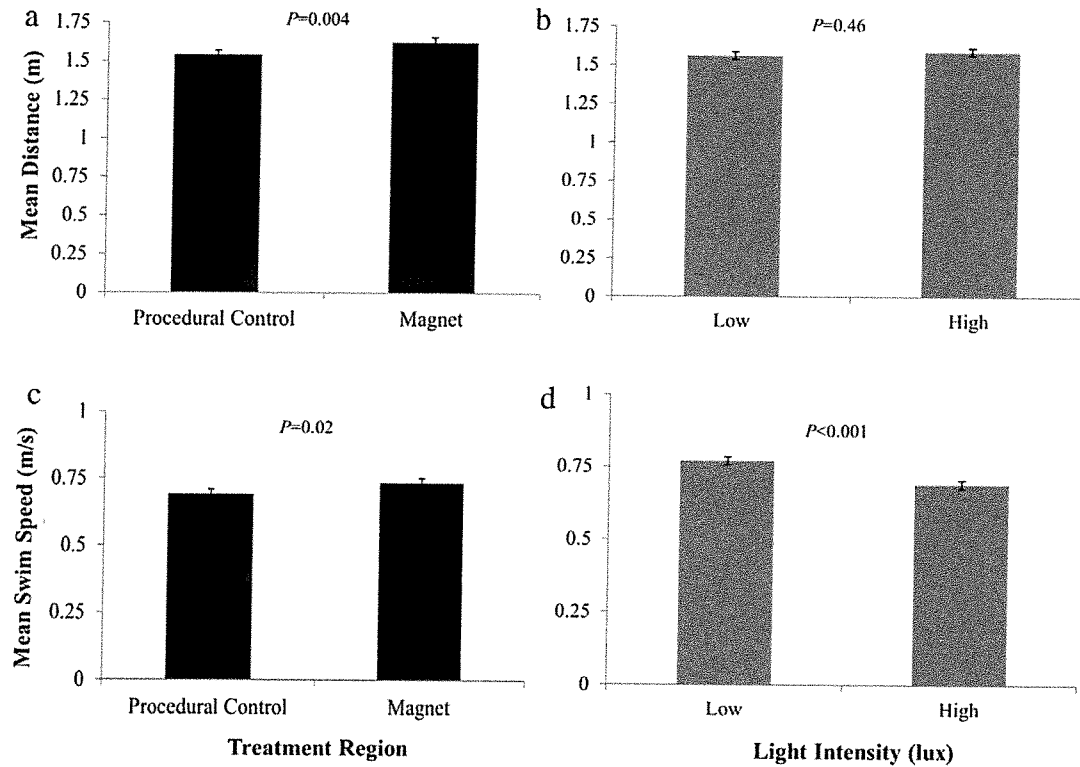
Fig. 5. The mean closest distance (±SE) (a, b) and mean swim speeds (±SE) (c, d) of bull sharks (*Carcharhinus leucas*) from the apparatus in relation to treatment region (a,c) and light intensity (b,d). The mean value of sea surface and seafloor light intensities for each trial is used as <1 lux as "Low" and ≥1 lux as "High".

3.3.2. Swim distance

Procedural control vs. magnetic. The mean distance (±SD) that *C. leucas* swam from the procedural control region was 1.54 m±0.42 and that from the magnetic region was 1.62 m±0.47. The difference between these was statistically significant (paired *t*-test; t = 2.89, d.f. = 212, *P* = 0.004), illustrating *C. leucas* swam at a significantly greater distance away from the magnetic treatment region in comparison to the procedural control region (Fig. 5a).

High vs. low light intensity. The mean distance (± SD) that *C. leucas* swam from the barrier during periods characterized by high and low light intensities were 1.59 m ± 0.48 and 1.56 m ± 0.43, respectively. This difference was not statistically significant (unpaired *t*-test; t = 0.75, d.f. = 678, *P* = 0.46), illustrating that distance from the barrier did not significantly vary with light intensity (Fig. 5b).

3.3.3. Swim speed

Procedural control vs. magnetic. The mean *C. leucas* swim speeds (± SD) in relation to the procedural control and magnetic regions were 0.69 m/s ± 0.25 and 0.74 m/s ± 0.25, respectively. This difference was statistically significant (paired *t*-test; t = 2.29, d.f. = 211, *P* = 0.02), illustrating that *C. leucas* swim speed was significantly greater in association with the magnetic region than that of the procedural control region (Fig. 5c).

High vs. low light intensity. The mean *C. leucas* swim speeds (± SD) during periods characterized by high and low light intensities were 0.69 m ± 0.28 and 0.77 m ± 0.21, respectively. Results demonstrate that this difference was statistically significant (unpaired *t*-test; t = 3.99, d.f. = 680, *P* < 0.001), illustrating that swim speed associated with periods of low light intensity was significantly greater than that of high light intensity (Fig. 5d).

4. Discussion

This study aimed to determine if the Sharksafe barrier could exclude *C. leucas* from bait. During the experiment, the swimming behavior of all interacting *C. leucas* (n ≥ 23) was manipulated in the presence of the procedural control and magnetic barrier regions, which was evidenced by an increase in avoidance and pass around frequencies, and a decrease in entrance frequencies in comparison to the control region. In fact, no *C. leucas* swam through the procedural control or magnetic regions, whereas sharks made 1260 entrances through the control region. Furthermore, significant behavioral differences in response to various factors such as conspecific density, heterospecific density, and light intensity illustrate how behavior can vary on a context-specific basis.

4.1. Basic behavioral interactions

4.1.1. Bull sharks

Comparable to previous studies, *C. leucas* behavior was significantly altered in relation to both the magnetic and procedural control regions (O'Connell et al., 2013b, 2014). In O'Connell et al. (2014), white sharks (*Carcharodon carcharias*) never entered through procedural control and magnetic regions of the Sharksafe barrier. Similarly, in O'Connell et al. (2013b), *C. leucas* were observed to swim around magnetic and procedural control regions of a barrier; however unlike the present study and O'Connell et al. (2014), entrance behaviors through procedural control and magnetically-treated barrier regions did occur. In the present study and in O'Connell et al. (2014), there were two and three rows of alternating columns, respectively, whereas in the previous study (O'Connell et al., 2013b), only one row of columns was deployed. Therefore, the added visual stimulus provided by increased column quantity may have been sufficient to elicit these behavioral differences and may have maximized overall barrier effectiveness. Secondly, inter-experimental differences in *C. leucas* behavior towards barrier structures may be a result of inter-column spacing variations. In O'Connell et al. (2013b), inter-column spacing was 1.5 m whereas inter-column spacing was 0.63 m in the present study when both alternating rows are considered. This reduction may be an influential factor since visual stimuli and magnetic field density were maximized. By maximizing magnetic field density, fewer magnetic field gaps existed between barrier columns and thus maximized the overall potential of *C. leucas* exposure and repellency. Beyond visual and magnetic stimuli, field observations revealed that tactile stimulation that occurred between sharks and the barrier might have provided an additional deterrent effect. Elasmobranchs have shown to possess mechanoreception capabilities (Boord and Campbell, 1977; Roberts, 1978; Kasumyan, 2003; Maruska and Tricas, 2004). This stimulation is perceived through hydrodynamic disturbances and/or direct tactile stimulation (e.g. Boord and Campbell, 1977; Maruska and Tricas, 2004). In the present study, there were eight occasions where *C. leucas* followed prey and made contact with the barrier. After initial contact, prey typically swam through the barrier whereas sharks were observed to exhibit violent avoidance behaviors (e.g. 180° turns and accelerations away). These findings illustrate that increased column density may provide increased tactile stimulation and overall barrier exclusion efficacy.

Besides entrance behaviors, avoidance behaviors were most frequent towards the magnetic region. These findings suggest that beyond the visual stimuli provided by the columns, the magnetic fields might have enhanced barrier exclusion efficacy, further supporting previous studies on magnetoreception capabilities and magnetic repellent effects on elasmobranchs (Rigg et al., 2009; O'Connell et al., 2010, 2011a, 2012a, 2013a,b).

Lastly, a significantly greater quantity of pass around behaviors occurred towards the procedural control and magnetic regions. Since elasmobranchs are characterized by having well developed eyes (Hart et al., 2004, 2006) and a large proportion of the brain is dedicated to visual information processing (Lisney and Collin, 2006) these visual stimuli provided by both treatment regions may have been sufficient to elicit this behavioral type.

4.1.2. Non-target species

Several other elasmobranch and teleost species were observed to interact with the barrier. Of these, only *N. brevirostris* exhibited similar behavioral exclusion with no entrances through procedural control and magnetic regions. However, findings differed for *G. cirratum, U. jamaicensis*, and *S. barracuda*. Interspecific behavioral differences towards barrier stimuli may be explained by a variety of organismal characteristics, such as behavioral patterns, body width, and presence/absence of ampullary receptors. For example, *G. cirratum* have differing behavioral habits (e.g. rest on sandy bottoms, caves, crevices—Compagno, 2001) than both *C. leucas* and *N. brevirostris*, which tend to be more mobile. Therefore, the observed lack of avoidance and increased entrance frequency in comparison to both *C. leucas* and *N. brevirostris* may be explained by behavioral traits and may further demonstrate a limitation pertaining to the overall exclusion capabilities of the barrier. Secondly, the *U. jamaicensis* (disc width ~20–30 cm), *G. cirratum* (body width ~30–61 cm) and *S. barracuda* (body width ~10–18 cm) that were observed in this study had a body width that was substantially smaller than the inter-column spacing (0.63 m). In comparison, the body width of *N. brevirostris* (~0.80–1.0 m) and *C. leucas* (~ 0.87–1.11 m) were substantially wider and therefore it is possible that this barrier also functions through physical exclusion where pectoral fin width or body width dictates entrance likelihood. Besides body width, the lack of avoidance in *S. barracuda* towards the magnetic region may be due to its lack of ampullary receptors.

4.2. Biological and environmental parameters

4.2.1. Animal density

Organisms that occupy a similar ecological niche and spatial resource often compete both within (i.e. intraspecific competition) and between (i.e. interspecific competition) species (Nelson and Johnson, 1980; Schoener, 1983), which have been demonstrated to alter behavior (Crombie, 1947; Nelson and Johnson, 1980; Polis, 1981; Stiling et al., 1984; Munday et al., 2001). In previous studies, increasing conspecific densities yielded increased depredation rates on repellent-associated hooks/baits (Brill et al., 2009; Jordan et al., 2011; Robbins et al., 2011). Similar to these studies, significant positive relationships between animal density and behavior were found. This suggests that animal density does influence *C. leucas* behavioral patterns. However, since no entrance behaviors were observed through procedural control and magnetic regions, the animal densities observed in this study are not considered to be a factor affecting overall barrier exclusion efficacy.

4.2.2. Light intensity

Throughout the experiment, light intensity changed; however, the effects of this change only had a significant influence on avoidance frequency. For sea surface (Upper) light intensity, there was an inverse relationship where an increase in light intensity characteristics yielded an overall decrease in avoidance behaviors. Such findings suggest that increased light intensity characteristics may give C. leucas a greater ability to visually perceive the barrier at greater distances. This increased visual perception may reduce magnetically-influenced avoidance behaviors or avoidance behaviors elicited by short-range visual detection or tactile stimulation associated with making contact with the barrier. This also suggests that decreased light intensity characteristics may yield increased avoidance. In many coastal environments classified as being highly turbid due to riverine input (Mulder and Syvitski, 1995), runoff (Crivelli et al., 1995), eutrophication Rosenberg, 1985; Smetacek et al., 1991, the use of magnetic barriers may result in increased barrier exclusion efficacy. Coincidentally, these are also areas where beach nets are currently deployed.

4.3. Application of the ARIS dual-frequency acoustic camera

This study demonstrates that the ARIS acoustic camera can be effectively and accurately used to estimate animal size, regardless of light intensity. These findings are consistent with previous studies employing lower frequency DIDSON sonar cameras (Holmes et al., 2006; Boswell et al., 2008; Han et al., 2009; Burwen et al., 2010; Becker et al., 2011; Langkau et al., 2012; Rakowitz et al., 2012). For example, Rakowitz et al. (2012) demonstrated that the DIDSON could be effectively used to define and understand heterogeneous behavioral fish patterns in response to trawling gears and additionally, how the technology accurately estimated fish abundance. Similarly, Becker et al. (2011) used DIDSON and revealed detailed characteristics of South African fish populations that highlighted how both biotic and abiotic factors can influence fish distribution and behavior. With the present findings and previous analyses, high resolution sonar technologies can be beneficial tools in effectively analyzing fish behavior and obtaining accurate measurements (e.g. size), especially in situations where surface observation is not possible and low light levels prevent the use of optical cameras.

However, although not significantly different, the quantified behaviors obtained during field observations and post hoc ARIS video analyses were not strictly 1:1 in the present study. These inaccuracies may be due to a variety of reasons. First, even when highly trained, it was difficult to accurately discern between N. brevirostris, G. cirratum and C. leucas during post hoc image analysis. Due to this, volunteers may have accidentally misidentified N. brevirostris and G. cirratum interactions as C. leucas interactions, which may have led to inflated behavioral quantities. Secondly, the horizontal capture angle was 30°. Therefore, the region of recordable behaviors that was closest to the camera ranged from 2 to 2.5 m and regions greater than 2–2.5 m were excluded from the camera frame. In contrast, field observations typically occurred at a maximum of 2.5–3 m from the barrier (e.g. dependent on shark body length). This distance variation between post hoc video and field analyses may have contributed to the deviation from 1:1. Thirdly, the ARIS camera has a maximum range of 20 m. The terminal part of the treatment region that was furthest from the ARIS camera was approximately 18–19 m, and therefore at the maximum range. At this distance, sharpness and resolution of animals swimming through the camera frame were reduced. This reduction in quality may have led to slightly inaccurate post hoc video analysis, which may have also contributed to the deviation from 1:1 in observation techniques.

Although behavioral observations were not exactly 1:1, the ARIS camera was beneficial for this research as previous magnetic-repellent analyses did not have the capabilities to conduct observations during low light intensity situations (e.g. O'Connell et al., 2012a, 2013b). Using this system, observing behaviors such as swim speed and distance away from treatments during both day and night was made possible. Throughout the experiment, swim speed was significantly higher near the magnetic region and during low light intensity situations (<1 lux). The swim speeds near the magnetic region may be directly correlated with the increase in avoidance behaviors towards this region. Avoidance behaviors were often characterized by brief accelerations and therefore, it is possible that the presence of the magnets may have increased C. leucas swim speed. In addition, the feeding activity of C. leucas is known to increase during nocturnal hours (Driggers et al., 2012; Brunnschweiler and Barnett, 2013). It is possible that the observed increase in swim speeds at night (e.g. periods of low light intensity) is directly correlated with foraging activity. In fact, observers recorded eight feeding attempts on Atlantic tarpon (Megalops atlanticus) which exclusively occurred during the night.

The distance that C. leucas swam from the magnetic region was significantly greater than that associated with the procedural control region. In context, this makes intuitive sense due to the associated magnetic fields; however, the magnetic flux that extends beyond 40–50 cm is similar to ambient geomagnetic fields and would not explain why the mean distance that sharks were swimming from the magnets was 1.62 m ± 0.47 since this was far outside the range of supernormal magnetic fields/fluxes. One plausible explanation for these findings is that avoidance behaviors were more common towards the magnetic region. These avoidances yielded turns or accelerations away from a treatment region and thus, an increased quantity of avoidances would inevitably yield to increased distance from a barrier region.

5. Conclusion

Both the procedural control and magnetic regions of the Sharksafe barrier can successfully exclude C. leucas from bait which has promising implications for future conservation applications, such as an eco-friendly alternative to beach nets.

Although only one subpopulation of *C. leucas* was studied, none of the *C. leucas* entered through either barrier region regardless of light intensity or the number of animals in the area. These findings illustrate promise for the utility of this barrier to effectively exclude this species regardless of time of day and/or level of conspecific and heterospecific density. Although the procedural control region had a similar exclusion effect on *C. leucas*, magnets have illustrated enhanced deterrent capabilities on many other shark species, including Caribbean reef (*Carcharhinus perezi*), great hammerhead (*Sphyrna mokarran*) and nurse (*Ginglymostoma cirratum*) sharks which illustrates the importance of magnetic inclusion in future experiments (O'Connell, 2013). Furthermore, although it could not directly be addressed due to the difficulties in re-identifying sharks throughout the experiment, indications of barrier stimuli habituation (e.g. closer approaches and/or increased frequency of entrance) were not observed which has implications for long-term barrier deployment. The present findings provide a strong foundation for continued research on other large sharks that pose a potential threat to beachgoers, such as *C. carcharias* and *G. cuvier*.

Acknowledgments

References

Anon,, 1998, The Queensland Shark Control Program: Report of the committee of review 1997. (Queensland Department of Primary Industries: Brisbane).

Bastian, J., 1994. Electrosensory organisms. Physics Today 47, 30–37.

Bates, D., Maechler, M., Bolker, B., 2012. lme4: Linear mixed-effects models using S4 classes. R package.

Becker, A., Whitfield, A.K., Cowley, P.D., Järnegren,, Næsje, T.F., 2011. An assessment of the size structure, distribution, and behavior of fish populations within a temporarily closed estuary using dual frequency identification sonar (DIDSON). J. Fish Biol. 9, 761–775.

Boord, R.L, Campbell, C.B.G., 1977. Structural and Functional Organization of the Lateral Line System of Sharks. Amer. Zoologist 17 (2), 431–441.

Boswell, K.M., Wilson, M.P., Cowan Jr., J.H., 2008. A semiautomated approach to estimating fish size, abundance, and behavior from dual-frequency identification sonar (DIDSON) data. N. Am. J. Fisheries Manage. 28, 799–807.

Brill, R., Bushnell, P., Smith, L., Speaks, C., Sundaram, R., Stroud, E., Wang, J., 2009. The repulsive and feeding deterrent effects of electropositive metals on juvenile sandbar sharks (*Carcharhinus plumbeus*). Fisheries Bull. 107, 298–307.

Brown, B.R., Hughes, M.E., Russo, C., 2005. Infrastructure in the electric sense: admittance data from shark hydrogels. J. Comparative Physiol. A 191, 115–123.

Brunnschweiler, J.M., Barnett, A., 2013. Opportunistic Visitors: Long-Term Behavioural Response of Bull Sharks to Food Provisioning in Fiji. PLoS ONE 8 (3), e58522. http://dx.doi.org/10.1371/journal.pone.0058522.

Burwen, D.L., Fleischman, S.J., Miller, J.D., 2010. Accuracy and precision of salmon length estimates taken from DIDSON sonar images. Trans. Amer. Fisheries Soc. 139, 1306–1314.

Compagno, L.J.V., 2001. Sharks of the world: An annotated and illustrated catalogue of shark species known to date. Food Agric. Organ. 2 (1), 269.

Crivelli, A.J., Ximenes, M.C., Gout, B., Lasserre, G., Freon, P., Do Chi, T., 1995, Causes and effects of terrestrial runoff and riverine outflow on brackish/coastal marine fisheries ecosystems in the northern Mediterranean region. In Effects of riverine inputs on coastal ecosystems and fisheries resources, FAO Fisheries Technical Paper 349, pp. 59–88.

Crombie, A.C., 1947. Interspecific competition. J. Anim. Ecol. 16 (1), 44–73.

Dobson, A.J., Barnett, A.G., 2008. An Introduction to Generalized Linear Models, Third edition. Chapman & Hall/CRC, Boca Raton.

Driggers III, W.B., Campbell, M.D., Hoffmayer, E.R., Ingram Jr., G.W., 2012. Feeding chronology of six species of carcharhinid sharks in the western North Atlantic Ocean as inferred from longline capture data. Marine Ecological Progress Series 465, 185–192. http://dx.doi.org/10.3354/meps09901.

Dudley, S.F.J., 1997. A comparison of the shark control programs of New South Wales and Queensland (Australia) and KwaZulu-Natal (South Africa). Ocean and Coastal Management 34, 1–27.

Dudley, S.F.J., Cliff, G., 1993. Some effects of shark nets in the Natal nearshore environment. Environ. Biol. Fishes 36, 243–255.

Dudley, S.F.J., Gribble, N.A., 1999, Case studies of the management of elasmobranch fisheries. Part 2. FAO Fisheries Technical Paper. 480–920.

Faraway, J.J., 2006. Extending the Linear Model with R: Generalized Linear, Mixed Effects and Nonparametric Regression Models. Chapman & Hall/CRC, Boca Raton.

Gribble, N.A., McPherson, G., Lane, B., 1998. Effect of the Queensland shark control program on non-target species: whale, dugong, turtle and dolphin: a review. Marine Freshwater Res. 49, 645–651.

Hamer, G., 1993, An overview of the New South Wales meshing program. In Shark Conservation (Proceedings of an International Workshop on the Conservation of Elasmobranchs, Sydney, Australia, 24 February 1991), Zoological Parks Board, Mosman, pp. 87–91.

Han, J., Honda, N., Asada, A., Shibata, K., 2009. Automated acoustic method for counting and sizing farmed fish during transfer using DIDSON. Fish. Sci. 75, 1359–1367.

Hart, N.S., Lisney, T.J., Collin, S.P., 2006. Visual communication in elasmobranchs. In: Fish communication, vol. 2. Science Publishers Inc, Enfield, pp. 337–392.

Hart, N.S., Lisney, T.J., Marshall, N.J., Collin, S.P., 2004. Multiple cone visual pigments and the potential for trichromatic colour vision in two species of elasmobranch. J. Exp. Biol. 207 (26), 4587–4594. http://dx.doi.org/10.1242/jeb.01314.

Hodson, R.B., 2000, Magnetoreception in the short-tailed stingray, *Dasyatis brevicaudata*, M.S. thesis, University of Auckland, Auckland, New Zealand.

Holmes, J.A., Cronkite, G.M.W., Enzenhofer, H.J., Mulligan, T.J., 2006. Accuracy and precision of fish-count data from a dual-frequency identification sonar (DIDSON) imaging system. ICES J. Mar. Sci. 63, 543–555.

Hyun, S.-Y., Cadrin, S.X., Roman, S., 2014. Fixed and mixed effect models for fishery data on depth distribution of Georges Bank yellowtail flounder. Fish. Res. 157, 180–186.

Jordan, L.J., Mandelman, J.W., Kajiura, S.M., 2011. Behavioral responses to weak electric fields and a lanthanide metal in two shark species. J. Exp. Mar. Biol. Ecol. 409, 345–350.

Kajiura, S.M., Holland, K.N., 2002. Electroreception in juvenile scalloped hammerhead and sandbar sharks. J. Exp. Biol. 205 (23), 3609–3621.

Kalmijn, A.J., 1966. Electro-perception in sharks and rays. Nature 212, 1232–1233.

Kalmijn, A.J., 1971. The electric sense of sharks and rays. J. Exp. Biol. 55, 371–383.

Kalmijn, A.J., 1973. Electro-orientation in sharks and rays: theory and experimental evidence. Scripps Inst. Oceanogr. 73 (39), 1–22.

Kalmijn, A.J., 1974. The detection of electric fields from inanimate and animate sources other than electric organs. In: Fessard, A. (Ed.), Electroreceptors and Other Specialized Receptors in Lower Vertebrates. In: Handbook of Sensory Physiology, vol. 3. Springer-Verlag, Berlin, Germany, pp. 147–200.

Kalmijn, A.J., 1982. Electric and magnetic field detection in elasmobranch fishes. Science 218, 916–918.

Kalmijn, A.J., 1984. Theory of electromagnetic orientation: a further analysis. In: Comparative Physiology of Sensory Systems. Cambridge University Press, New York, pp. 525–560.

Kalmijn, A.J., 2000. Detection and processing of electromagnetic and near-field acoustic signals in elasmobranch fishes. Philos. Trans. R. Soc. London B 355, 1135–1141.

Kasumyan, A.O., 2003. The lateral line in fish: Structure, function and role in behaviour. J. Ichthyol. 43, S175–S203.

Klimley, A.P., 1993. Highly directional swimming by scalloped hammerhead sharks, Sphyrna lewini, and subsurface irradiance, temperature, bathymetry, and geomagnetic field. Marine Biol. 117, 1–22.

Klimley, A.P., Beavers, S.C., Curtis, T.H., Jorgensen, S.J., 2002. Movements and swimming behavior of three species of sharks in La Jolla Canyon, California. Environ. Biol. Fishes 63, 117–135.

Langkau, M.C., Balk, H., Schmidt, M.B., Borcherding, J., 2012. Can acoustic shadows identify fish species? A novel application of imaging sonar data. Fish. Manag. Ecol. 19, 313–322.

Lisney, T.J., Collin, S.P., 2006. Brain morphology in large pelagic fishes: a comparison between sharks and teleosts. J. Fish Biol. 68 (2), 532–554. http://dx. doi.org/10.1111/j.0022-1112.2006.00940.

Maruska, K.P., Tricas, T.C., 2004. Test of the mechanotactile hypothesis: neuromast morphology and response dynamics of mechanosensory lateral line primary afferents in the stingray. J. Exp. Biol. 207, 3463–3476.

Meyer, C.G., Holland, K.N., Papastamatiou, Y.P., 2005. Sharks can detect changes in the geomagnetic field. Journal of the Royal Society Interface 2, 129–130.

Molteno, T.C.A., Kennedy, W.L., 2009. Navigation by Induction-Based Magnetoreception in Elasmobranch Fishes. Journal of Biophysics 2009 (380976), 6. http://dx.doi.org/10.1155/2009/380976.

Mulder, T., Syvitski, J.P.M., 1995. Turbidity currents generated at river mouths during exceptional discharges to the world oceans. Journal of Geology 103 (3), 285–299.

Munday, P.L., Jones, G.P., Caley, M.J., 2001. Interspecific competition and coexistence in a guild of coral-dwelling fishes. Ecology 82, 2177–2189.

Nelson, D.R., Johnson, R.H., 1980. Behavior of the reef sharks of Rangiroa, French Polynesia. National Geographic Society Research Reports 12, 479–498.

O'Connell, C.P., 2013. The Effect of Biological and Environmental Factors on Elasmobranch Magnetoreception and its Application for Conservation in Beach Nets and Fishing Gears. University of Massachusetts Dartmouth. Dissertation.

O'Connell, C.P., Abel, D.C., Rice, P.H., Stroud, E.M., Simuro, N.C., 2010. Responses of the Southern Stingray (Dasyatis americana) and the Nurse Shark (Ginglymostoma cirratum) to Permanent Magnets. Marine and Freshwater Behavior and Physiology 43, 63–73.

O'Connell, C.P., Abel, D.C., Stroud, E.M., 2011b. Analysis of permanent magnets as elasmobranch bycatch reduction devices in hook-and-line and longline trials. Fish. Bull. 109 (4), 394–401.

O'Connell, C.P., Andreotti, S., Rutzen, M., Meyer, M., He, P., 2012a. The use of permanent magnets to reduce elasmobranch encounter with a simulated beach net. 2. The great white shark (Carcharodon carcharias) Ocean and Coastal Management. http://dx.doi.org/10.1016/j.ocecoaman.2012.11.006. Special Issue.

O'Connell, C.P., Andreotti, S., Rutzen, M., Meyer, M., Matthee, C.A., He, P., 2014. Effects of the Sharksafe barrier on great white shark (Carcharodon carcharias) behavior and its implication for future conservation technologies. Journal of Experimental Marine Biology and Ecology 460, 37–46.

O'Connell, C.P., Gruber, S.H., Abel, D.C., Stroud, E.M., Rice, P.H., 2011a. The responses of juvenile lemon sharks, Negaprion brevirostris, to a magnetic barrier. Ocean and Coastal Management 54 (3), 225–230.

O'Connell, C.P., Gruber, S.H., O'Connell, T.J., Johnson, G., Grudecki, K., He, P., 2013b. The use of permanent magnets to reduce elasmobranch encounter with a simulated beach net. 1. The Bull Shark (Carcharhinus leucas). Ocean and Coastal Management http://dx.doi.org/10.1016/j.ocecoaman.2013.12.012.

O'Connell, C.P., Guttridge, T.L., Brooks, J., Finger, J.S., Gruber, S.H., He, P., 2013a. Behavioral modification of visually deprived lemon sharks (Negaprion brevirostris) towards magnetic fields. Journal of Experimental Marine Biology and Ecology.

O'Connell, C.P., He, P., Joyce, J., Stroud, E.M., Rice, P.H., 2012b. Effects of the SMART Hook™(Selective Magnetic and Repellent-Treated Hook) on Spiny Dogfish Catch in the Gulf of Maine. Ocean Coast. Manag. http://dx.doi.org/10.1016/j.ocecoaman.2012.08.002.

Paulin, M.G., 1995. Electroreception and the compass sense of sharks. Journal of Theoretical Biology 174, 325–339.

Polis, G.A., 1981. The evolution and dynamics of intraspecific predation. Annual Review of Ecological Systems 12, 225–251.

Rakowitz, G., Tušer,, Řiha, M., Jůza, T., Balk, H., Kubečka, J., 2012. Use of high-frequency imaging sonar (DIDSON) to observe fish behavior towards a surface trawl. Fish. Res. 123–124, 37–48.

Rigg, D.P., Peverell, S.C., Hearndon, M., Seymour, J.E., 2009. Do elasmobranch reactions to magnetic fields in water show promise for bycatch mitigation?. Marine and Freshwater Research 60, 942–948.

Robbins, W.D., Peddemors, V.M., Kennelly, S.J., 2011. Assessment of permanent magnets and electropositive metals to reduce the line-based capture of Galapagos sharks, Carcharhinus galapagensis. Fish. Res. 109, 100–106.

Roberts, B.L., 1978. Mechanoreceptors and the behaviour of elasmobranch fishes with special reference to the acoustico-lateralis system. In: Sensory biology of sharks, skates, and rays. Arlington, VA: Office of Naval Research. pp 331–390.

Rosenberg, R., 1985. Eutrophication—the future marine coastal nuisance? Marine Poll. Bull. 16, 227–231.

Schoener, T.W., 1983. Field experiments on interspecific competition. Amer. Nat. 122 (2), 240–285.

Sisneros, J.A., Tricas, T.C., Luer, C.A., 1998. Response properties and biological function of the skate electrosensory system during ontogeny. Journal of Comparative Physiology A 183, 87–99.

Smetacek, V., Bathmann, U., Nothig, E.M., Scharek, R., 1991. Coastal eutrophication: causes and consequences. In: Ocean Margin Processes in Global Change. Wiley, New York, pp. 251–279.

Stiling, P.D., Brodbeck, B.V., Strong, D.R., 1984. Intraspecific competition in Hydrellia valida (Diptera: Ephydridae), a leaf miner of Spartina alterniflora. Ecology. 65 (2), 660–662.

Stoner, A.W., Kaimmer, S.M., 2008. Reducing elasmobranch bycatch: laboratory investigation of rare earth metal and magnetic deterrents with spiny dogfish and Pacific halibut.. Fish. Res. 92, 162–168.

Tricas, T.C., Michael, S.W., Sisneros, J.A., 1995. Electrosensory optimization to conspecific phasic signals for mating. Neuroscience Letters 202, 129–132.

Tricas, T.C., Sisneros, J.A., 1995. Ecological functions and adaptations of the elasmobranch electrosense. In: Wiltschko, R., Wiltschko, W. (Eds.), The Senses of Fish: Adaptations for the Reception of Natural Stimuli, Narosa Publishing House, New Delhi. In: Magnetic Orientation in Animals, Springer Verlag, Berlin, pp. 308–329.